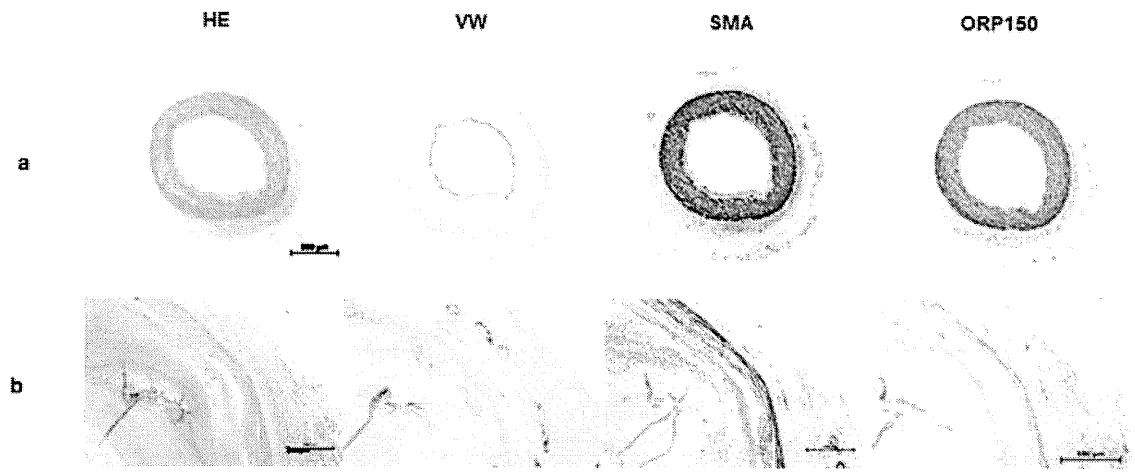

FIGURE 1. The media layer is hypoxic in normal arteries. (a) In a normal artery, von Willebrand factor (VWF) (endothelial cell marker) is clearly detected in the endothelium/intima and SMA (SMC marker) is homogenously present in the media. ORP150 (a marker of hypoxia) is detected in the media stained by SMA. (b) In a calcified artery, little VWF is detected, suggesting damage to the endothelial cells. The area stained by SMA is limited to the outer part of the media. ORP150 is also barely observed. These findings are opposite to those of the normal artery. Bars = 500 μm.

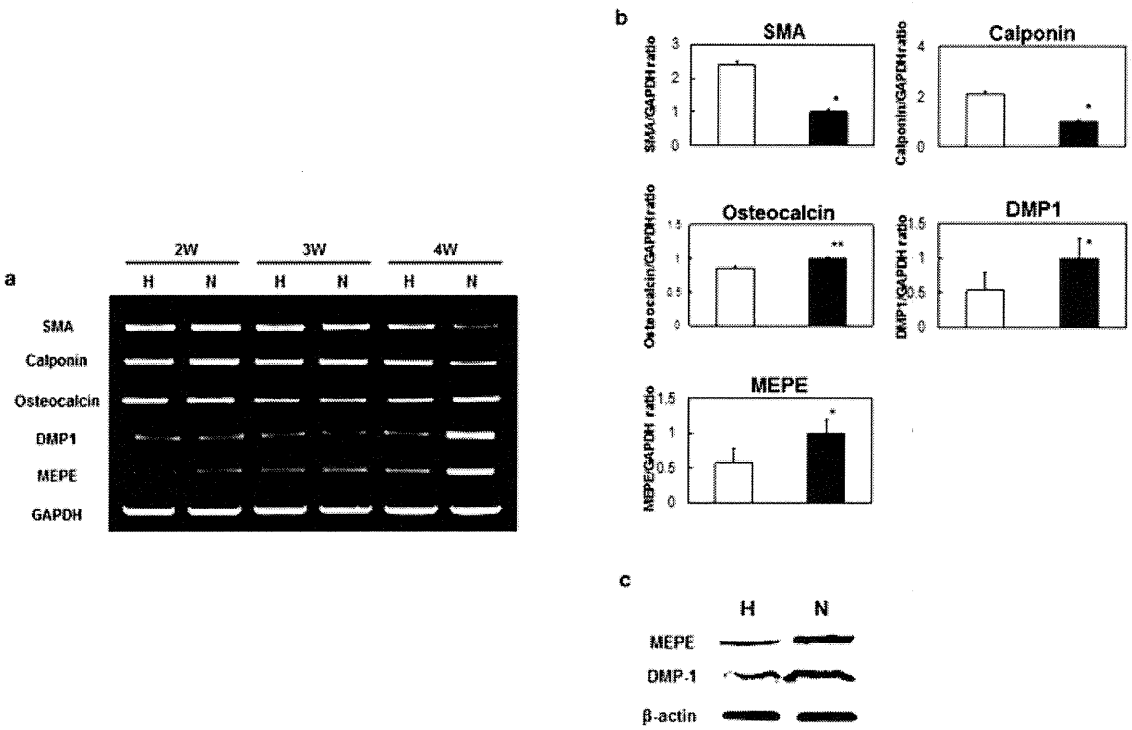

FIGURE 2. Hypoxia maintains a normal VSMC phenotype, whereas normoxia transforms VSMCs into osteogenic cells. (a) Total RNA was extracted from VSMCs cultured under hypoxic or normoxic conditions for 2, 3, and 4 weeks, and expression of mRNA for SMA, calponin (SMC marker), osteocalcin, and glyceraldehyde 3-phosphate dehydrogenase was analyzed by RT-PCR. (b) Quantification of SMA, calponin, osteocalcin, osteocalcin, DMP1, and MEPE gene expression by RT-PCR. Data are mean ± SD ($n = 3$) of the ratio of SMA, calponin, and osteocalcin gene expression under hypoxia compared with normoxia. $^{*}p < 0.001$, $^{**}p < 0.05$ (Mann–Whitney U test). □: Hypoxia, ■: Normoxia. (c) VSMCs were cultured under hypoxic and normoxic conditions for 4 weeks, followed by harvesting and lysis for Western blot analysis. H: hypoxia, N: normoxia

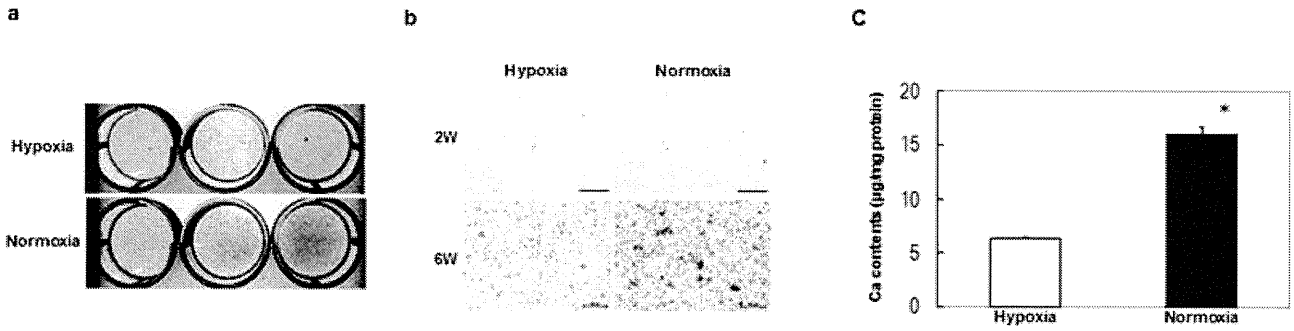

FIGURE 3. Hypoxia suppresses ALP activity and calcification of SMCs. (a) Human VSMCs stained for ALP after 2 weeks of culture. (b) VSMC cultures were stained with von Kossa stain after 2 or 6 weeks of incubation. (c) Calcium deposition was quantified at 6 weeks. Data are mean ± SD ($n = 3$). $^*p < 0.001$(Mann–Whitney U test).

REFERENCES

1. Owens G. Regulation of differentiation of vascular smooth muscle cells. Phys Rev 1995;75:487–517.
2. Schinke T, McKee MD, Karsenty G. Extracellular matrix calcification: where is the action? Nat Genet 1999;21:150–151.
3. Boström K. Cell differentiation in vascular calcification. Z Kardiol 2000;89(Suppl 2):II-69–II-74.
4. Boström K, Watson KE, Horn S, Wortham C, Herman IM, Demar LL. Bone morphogenetic protein expression in human atherosclerotic lesions. J Clin Invest 1993;91:1800–1809.
5. Hirao M, Tamai N, Tsumaki N, Yoshikawa H, Myoui A. Oxygen tension regulates chondrocyte differentiation and function. J Biol Chem 2006;181:31079–31092.
6. Nishizawa Y, Jono S, Ishimura E, Shioi A. Hyperphosphatemia and vascular calcification in end-stage renal disease. J Ren Nutr 2005;15:178–182.
7. Proudfoot D, Davies JD, Skepper JN, Weissberg PL, Shanahan CM. Acetylated low-density lipoprotein stimulates human vascular smooth muscle cell calcification by promoting osteoblastic differentiation and inhibiting phagocytosis. Circulation 2002;106:3044–3050.
8. Parhami F, Morrow AD, Balucan J, Leitinger N, Watson AD, Tintut Y, Berliner JA, Demar LL. Lipid oxidation products have opposite effects on calcifying vascular cell and bone cell differentiation. A possible explanation for the paradox of arterial calcification in osteoporotic patients. Arterioscler Thromb Vasc Biol 1997;17:680–687.
9. Mody N, Parhami F, Sarafan TA, Demar LL. Oxidative stress modulates osteoblastic differentiation of vascular and bone cells. Free Radic Biol Med 2001;31:509–519.

Treatment of Partial Growth Arrest Using an In Vitro-generated Scaffold-free Tissue-engineered Construct Derived From Rabbit Synovial Mesenchymal Stem Cells

Kiyoshi Yoshida, MD, Chikahisa Higuchi, MD, PhD, Akio Nakura, MD, PhD, Norimasa Nakamura, MD, PhD, and Hideki Yoshikawa, MD, PhD

Background: Injuries to the epiphyseal plate sometimes result in partial growth arrest, which can lead to the development of angular deformities and limb length discrepancies in growing children. The aim of this study was to develop a new treatment for partial growth arrest of the physis. For this purpose, we investigated the feasibility of an in vitro-generated scaffold-free tissue-engineered construct (TEC) derived from synovial mesenchymal stem cells (MSCs) in a rabbit growth arrest model.

Methods: An experimental model for growth arrest was created by excising the medial half of the proximal growth plate of tibias from 6-week-old New Zealand White rabbits. Three experimental groups were set to evaluate TEC implantation: group 1, no implantation as controls; group 2, implantation of bone wax as additional controls; and group 3, implantation of TEC in the lesion.

Results: In group 1, all damaged growth plates were arrested and angular deformities appeared 4 weeks later. In groups 2 and 3, angular deformities were less than in the control group. Histologic images showed bone bridges developed at the damaged growth plate in group 1. Regeneration of growth plates was recognized in groups 2 and 3. Histologic examination showed greater regeneration of the growth plate in group 3 than in group 2. In addition, MSCs in the TEC differentiated into proliferative and prehypertrophic chondrocyte-like cells.

Conclusions: A scaffold-free 3D TEC made using cultured synovium-derived MSCs differentiated into proliferative and prehypertrophic chondrocyte-like cells.

Clinical Relevance: The results of this experimental study suggest that scaffold-free 3D TEC made using cultured synovium-derived MSCs can be a new approach for the repair of epiphyseal injury. Clinical effectiveness of a scaffold-free 3D TEC for growth arrest remains to be determined.

From the Department of Orthopaedic Surgery, Osaka University Graduate School of Medicine, Osaka, Japan.

This work was partially supported by the grant of Japan Orthopaedics and Traumatology Foundation Inc. No funds were used for salaries.

The authors declare no conflict of interest.

Reprints: Chikahisa Higuchi, MD, PhD, Department of Orthopaedic Surgery, Graduate School of Medicine, Osaka University, 2-2 Yamadaoka, Suita, Osaka 565-0871, Japan. E-mail: c-higuchi@umin.ac.jp.

Key Words: epiphyseal plate, physeal growth arrest, mesenchymal stem cell, tissue-engineered construct (TEC)

(*J Pediatr Orthop* 2012;32:314–321)

Injuries to the epiphyseal plate sometimes result in partial growth arrest, which can lead to the development of angular deformities and limb length discrepancies in growing children. Langenskiold[1,2] first demonstrated the prevention of growth arrest of the epiphyseal plate by physeal bridge resection and subsequent free transplant of fat in 1967. Since those reports, implantation of soft tissues including fat,[2–5] silastic,[6,7] and bone wax[3] have been investigated, and certain positive effects have been confirmed. However, those procedures may show limitations in terms of the control of bone growth and of the long-term safety of implant materials in vivo.

Stem cell therapies have focused on facilitating regenerative tissue repair of various tissues and organs. Among several cell sources, mesenchymal stem cells (MSCs) have the capability to differentiate into a variety of connective tissue cells, including bone, cartilage, tendon, and muscle.[8] These cells may be isolated from various tissues, such as bone marrow, skeletal muscle, and synovial membrane.[8–11] In addition to the selection of a cell source, finding an appropriate scaffold that provides a favorable 3-dimensional environment for cell proliferation and differentiation is important. For this purpose, many studies have placed priority on the development of scaffolds and various scaffolds have been approved for clinical use.[12] However, several issues associated with long-term safety remain. To minimize the risks involved, scaffold-free cell delivery systems may offer an excellent alternative.

Meanwhile, the unique matrix organization of articular cartilage results in antiadhesive properties that present an obstacle to the integration of tissues implanted adjacent to the cartilage matrix in the treatment of chondral injuries.[13] To overcome this problem, most implantation procedures into chondral lesions have required enzymatic treatment of the cartilage matrix surface,[14] or reinforcement of the initial fixation by sutures[15,16] or absorbable pins.[17] However, an animal study revealed

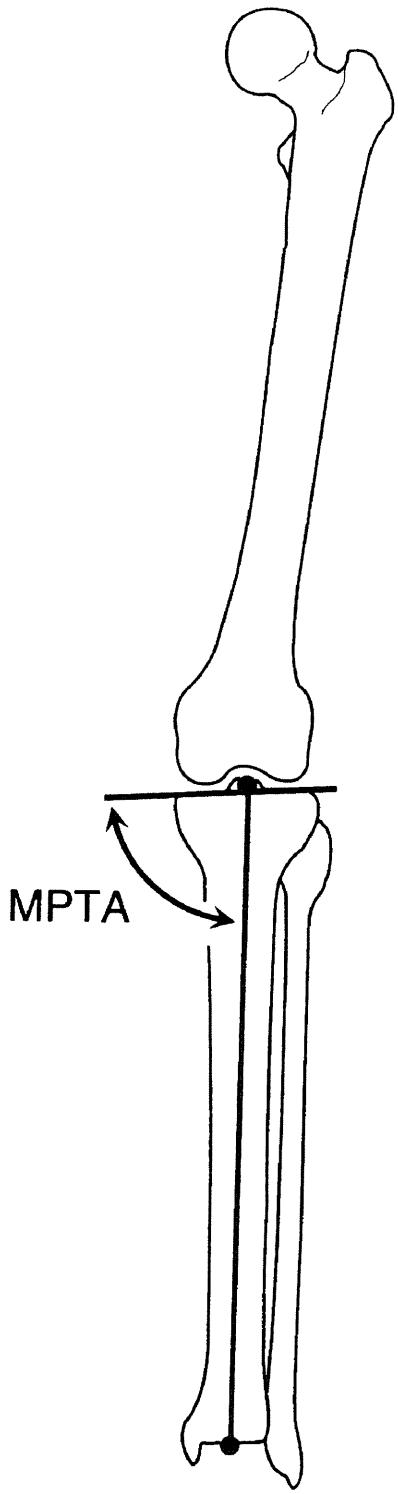

FIGURE 1. Medial proximal tibial angle (MPTA).

that suture tracks in the surrounding articular cartilage remain unhealed, representing a defect that could potentially act as a trigger site for subsequent matrix degradation around the margin between the implant and the adjacent cartilage tissue.[16] Implantable tissues that possess highly adhesive properties to cartilage tissue are thus needed for secure tissue integration.

We recently described the development of a scaffold-free 3-dimensional (3D) tissue-engineered construct (TEC) comprising MSCs derived from synovium and extracellular matrix synthesized by the cells.[18] Development of a 3D construct without the use of any artificial materials could be a key advantage for TECs. Implantation of a TEC into chondral defects in porcine knee joints initiated repair with a chondrogenic-like tissue, showing secure tissue integration with adjacent cartilage tissue.[18,19] Implantation of the TEC could thus be feasible to repair a damaged epiphyseal plate, based on the capacity for chondrogenic and osteogenic differentiation and high tissue adhesiveness.

The aim of the present study was thus to investigate the feasibility of using a TEC to repair damaged epiphyseal plates in a rabbit model.

TABLE 1. Histologic Grading Scale

Grade	Description
Cell morphology	
2	Columnar cartilage cells
1	Disordered cartilage cells
0	Noncartilage only
Staining (safranin O)	
3	
2	Slightly reduced
1	Significantly reduced
1	No staining
Thickness of epiphyseal plate*	
4	> 100%
3	75%-100%
2	50%-74%
1	25%-49%
0	< 25%

*Mean thickness of the repaired epiphyseal plate compared with that of the unoperated side.

METHODS

All procedures in this study followed the principles of the Declaration of Helsinki.

Harvest of Synovial Tissue and Isolation of MSCs

Synovial tissue was harvested from the knee joints of New Zealand White rabbits. Cells were isolated according to a previously reported protocol for the isolation of human synovial-derived MSC. Briefly, synovial membrane specimens were rinsed with phosphate-buffered saline (PBS), minced meticulously, and digested with 0.1% collagenase IV (Sigma, St Louis, MO) for 2 hours at 37°C. After neutralization of the collagenase with growth medium comprising high-glucose Dulbecco's modified Eagle's medium (DMEM; Gibco BRL, Life Technologies, Rockville, MD) supplemented with 10% fetal bovine serum (Hyclone, Logan, UT) and 1% penicillin/streptomycin (Gibco BRL, Life Technologies), cells were collected by centrifugation, washed with PBS, resuspended in the growth medium, and plated in culture dishes.

TABLE 2. MPTA at 4 Weeks After Surgery

Group 1	Group 2 (Bone Wax)	Group 3 (TEC)
62	70	74
64	76	76
64	80	79
65	83	80
75	90	84
—	—	85
—	—	88
66.0	79.8	80.9

MPTA indicates medial proximal tibial angle; TEC, tissue-engineered construct.

For expansion, cells were cultured in the growth medium at 37°C in a humidified atmosphere of 5% CO_2. The medium was replaced once a week. After 15 to 28 days of primary culture, when cells reached confluence, they were washed twice with PBS, harvested by treatment with trypsin-EDTA (0.25% trypsin and 1 mM EDTA; Gibco BRL, Life Technologies), and replaced at a 1:3 dilution when cultures reached near confluence. Cells from passages 4 to 7 were used in the present study.

Development of Scaffold-free 3D TECs

TECs were developed using the previously reported method.[18–20] Synovial MSCs were plated onto culture dishes at a density of $4.0 \times 10^5/cm^2$ in the growth medium containing 0.2 mM ascorbate 2-phosphate. After 7 to 14 days in culture, a complex of cultured cells and the extracellular matrix synthesized by the cells was detached from the substratum by application of shear stress using gentle pipetting. The detached complex was left in suspension to form a 3D structure by active tissue contraction. This tissue represented a basic scaffold-free 3D TEC.

Creation of Partial Growth Arrest and Implantation of the TEC

Male 6-week-old New Zealand White rabbits were selected because these animals would have open physes for 4 to 6 months. Rabbits were operated under general anesthesia using intramuscular injection of ketamine

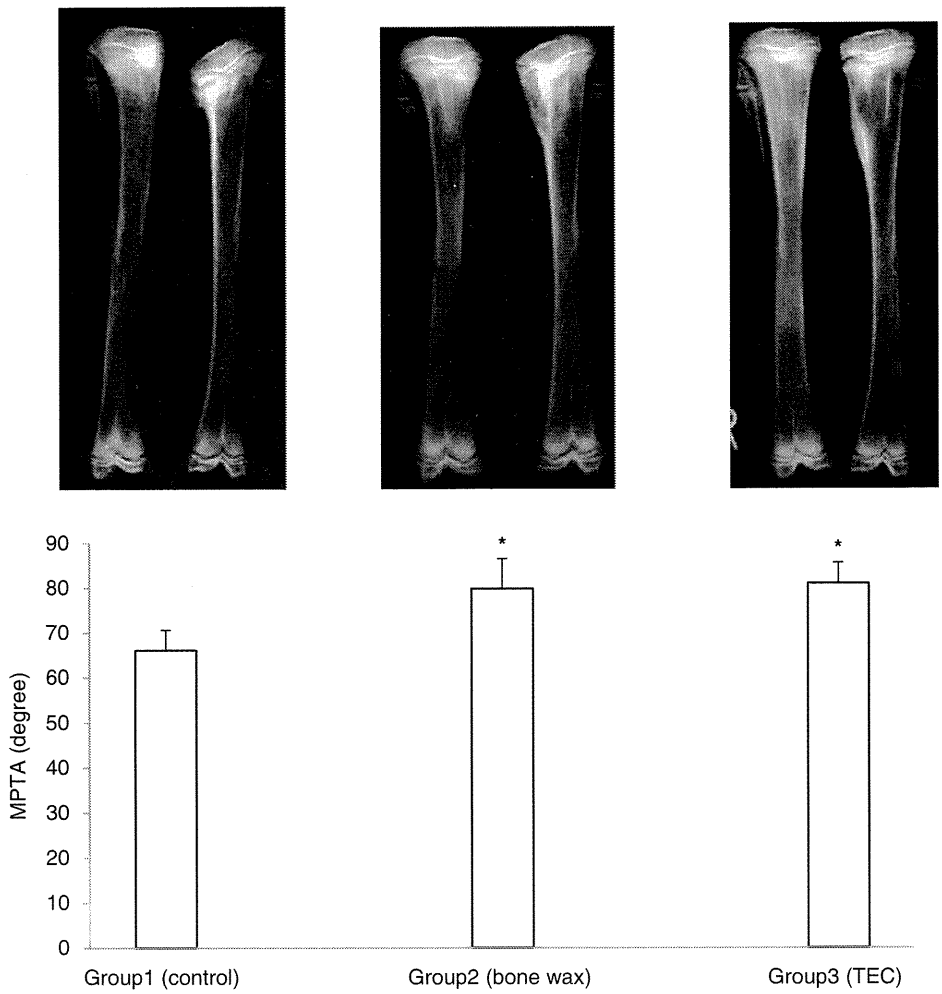

FIGURE 2. Medial proximal tibial angle (MPTA) at 4 weeks after surgery. Group 1 (control) showed varus deformity. Varus deformities were significantly better in groups 2 (bone wax) and 3 (TEC) than in group 1. *$P < 0.05$.

TABLE 3. MPTA at 8 Weeks After Surgery

Group 1	Group 2 (Bone Wax)	Group 3 (TEC)
37	56	56
41	58	59
45	65	61
47	69	65
65	73	80
—	—	88
47.0	64.2	68.2

MPTA indicates medial proximal tibial angle; TEC, tissue-engineered construct.

hydrochloride (30 mg/kg of body weight) and intravenous injection of propofol (80 mg/kg). The proximal part of the left tibia was exposed through an anteromedial incision. A window in the medial side of the growth plate was first made using a high-speed dental burr (diameter, 2 mm). The drill was then introduced and passed centrally into the epiphyseal growth plate region. Physeal defects of 3 mm diameter and 5 mm depth were created. The periosteum, subcutaneous tissue, and skin were then closed in layers. Rabbits were allowed free, weight-bearing movement with no immobilization of the legs. Operated rabbits were randomly divided into 3 groups as follows:

Group 1: nothing embedded into the physeal defect (n = 5).

Group 2: bone wax embedded into the physeal defect (n = 5).

Group 3: TECs were implanted into the physeal defect (n = 7).

Evaluation of TEC Effectiveness

Rabbits in all groups were killed at 4 or 8 weeks postoperatively. For radiographic evaluation, radiographs of the right (unoperated) and the left (operated) tibias were taken, and the medial proximal tibial angle (MPTA) was measured (Fig. 1).

For histologic evaluation, sections through the proximal tibia were made and stained with hematoxylin and eosin or safranin O. Histologic findings were scored according to a histologic grading scale (Table 1), with

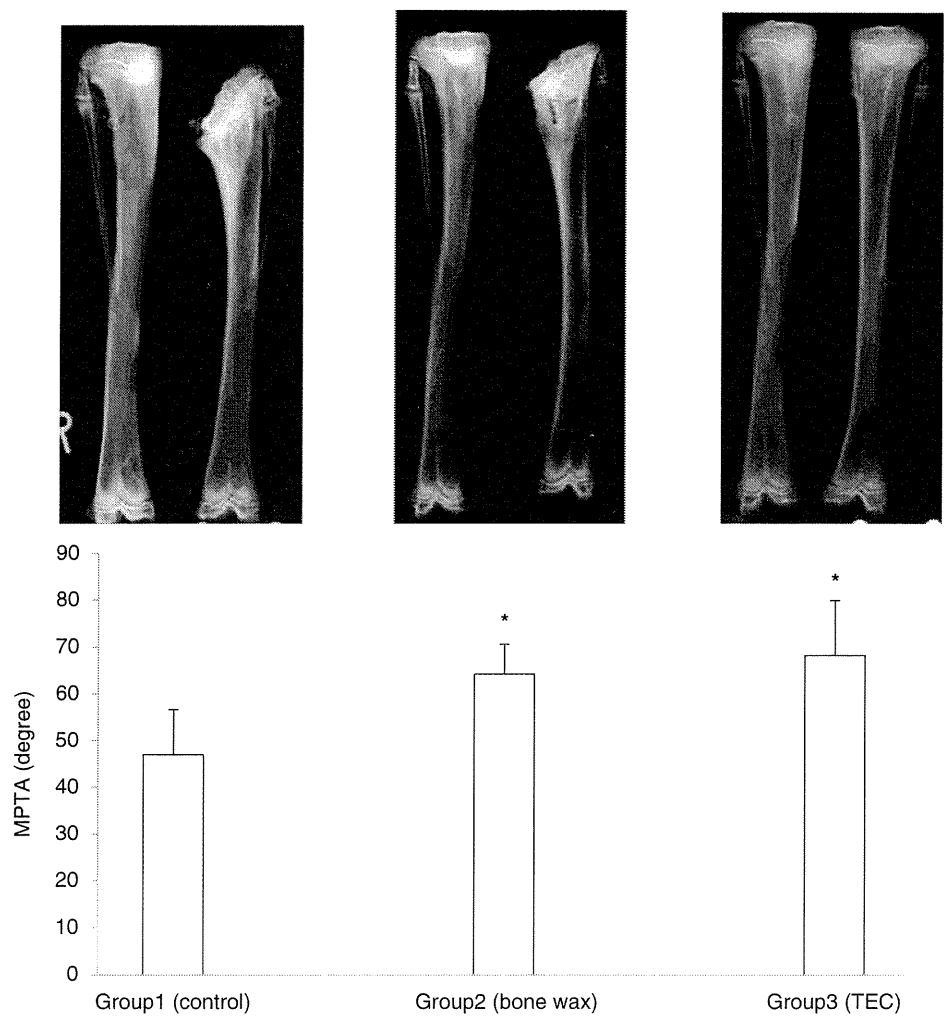

FIGURE 3. Medial proximal tibial angle (MPTA) at 8 weeks after surgery. Varus deformities were more severe in all groups than at 4 weeks. Varus deformities were significantly better in groups 2 (bone wax) and 3 (TEC) than in group 1. *$P < 0.05$.

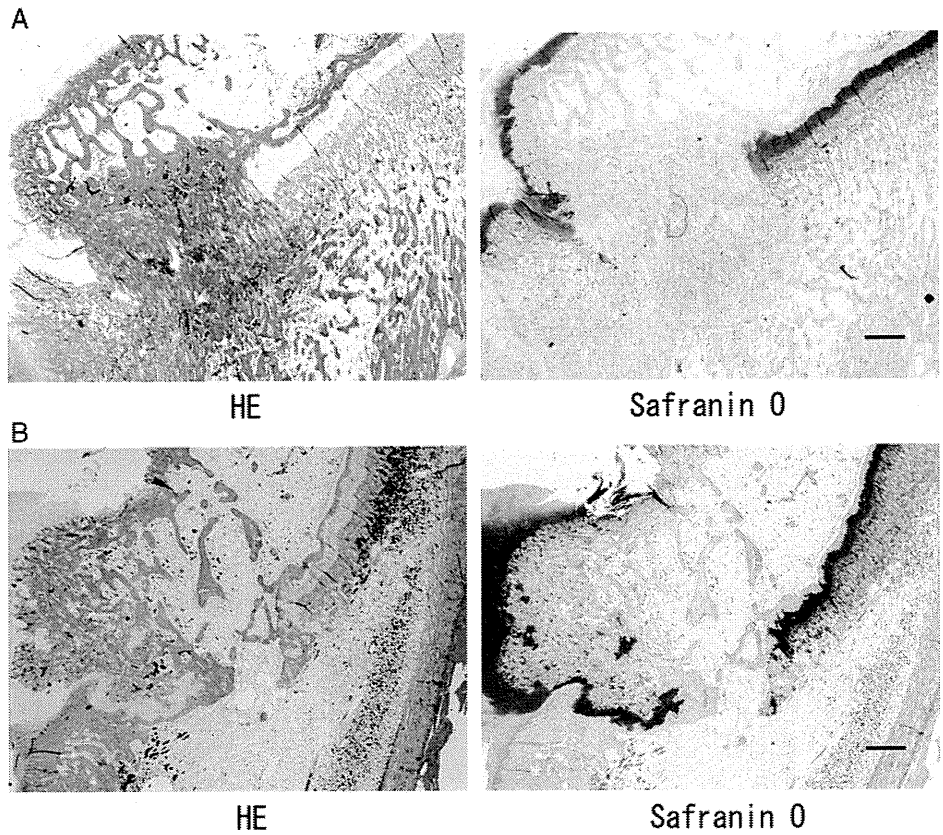

FIGURE 4. Histology in group 1. A, Histology at 4 weeks after surgery, showing bony bridge formation. B, Histology at 8 weeks. Bony bridge formation is increased and the epiphysis shows a wide connection with the metaphysis. Bar, 500 μm. HE indicates hematoxylin and eosin.

higher scores indicating higher quality of the growth plate repair.

Statistical Analysis

All data from at least duplicate samples are expressed as means ± SD, and a minimum of 3 independent experiments were performed. Unpaired Student *t* test or analysis of variance for multiple comparisons were used for statistical analysis. Differences between experimental groups were considered significant for values of $P < 0.05$.

RESULTS

Radiographic Results

Group 1 demonstrated angular deformity of the left tibia, with a mean MPTA of 66.0 degrees (range, 62 to 75 degrees) at 4 weeks after surgery (Table 2 and Fig. 2) and 47.5 degrees (range, 37 to 65 degrees) at 8 weeks after surgery (Table 3 and Fig. 3). Radiography in this group showed partial growth arrest of the proximal medial tibias (Figs. 2, 3). The mean MPTA of the right tibia was 88.0 degrees.

The mean MPTA in group 2 was 79.8 degrees (range, 70 to 90 degrees) at 4 weeks after surgery (Table 2 and Fig. 2) and 64.2 degrees (range, 56 to 73 degrees) at 8 weeks after surgery (Table 3 and Fig. 3). Varus deformity was milder than in group 1 at 4 weeks, postoperatively (Fig. 2). At 8 weeks after surgery, all cases showed varus deformity (Table 3 and Fig. 3). MPTA was significantly better than in group 1 at both 4 and 8 weeks after surgery (Figs. 2, 3).

The mean MPTA in group 3 was 80.9 degrees (range, 74 to 88 degrees) at 4 weeks after surgery (Table 2 and Fig. 2) and 68.2 degrees (range, 56 to 88 degrees) at 8 weeks after surgery (Table 3 and Fig. 3). Varus deformity was much milder than in group 1 at 4 weeks after surgery (Fig. 2), and MPTA in 3 of the 6 operated tibias was almost the same as in the unoperated tibias (Table 2). At 8 weeks postoperatively, 1 of the 6 operated tibias showed normal MPTA, and another case showed very little varus deformity. However, 4 of the 6 operated tibias showed varus deformity (Table 3 and Fig. 3). Compared with group 1, MPTA was significantly improved at both 4 and 8 weeks after surgery (Figs. 2, 3).

Histologic Findings

In group 1, a bony bridge formation replaced the epiphyseal growth plate at the operated site, with the epiphysis showing a wide connection with the metaphysis at 4 weeks after surgery (Fig. 4A) and increased connection at 8 weeks (Fig. 4B).

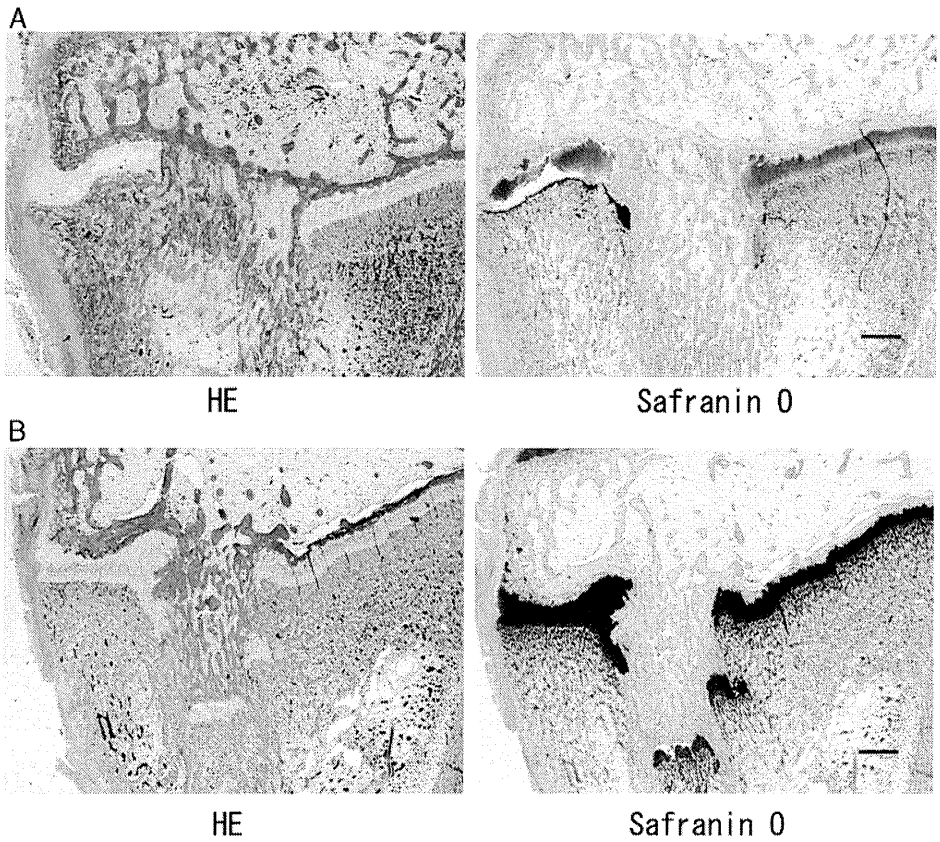

FIGURE 5. Histology in group 2 (bone wax). A, Histology at 4 weeks after surgery, showing partial bony bridge formation. B, Histology at 8 weeks, showing partial growth arrest over a wider area than at 4 weeks. Bar, 500 μm. HE indicates hematoxylin and eosin.

In group 2, all cases showed partial bony bridge formation. The transplanted bone wax remained at the operated site and showed no staining with hematoxylin and eosin or safranin O. However, some cases showed disappearance of transplanted bone wax and replacement with a bony bridge and growth plate-like tissue (Fig. 5). At 8 weeks after surgery, many cases showed a wider bony bridge area than at 4 weeks.

In group 3, all cases showed partial bony bridge formation. However, proliferative and prehypertrophic chondrocyte-like cells were seen at the operated site 4 weeks postoperatively (Fig. 6A). The cells took on a columnar arrangement like a normal physis and the physeal area was thickened (Fig. 6B). The cartilage matrix showed staining with safranin O, indicating the chondrogenic potential of MSCs in the TEC. Regeneration of the growth plate was recognized in the tibias without deformity (Fig. 6D).

Histologic Scores

Histologic findings at 4 and 8 weeks after surgery were evaluated and rated using a histologic grading scale (Table 1). At 4 weeks after surgery, histologic scores for the repaired growth plate were higher in groups 2 and 3 than in group 1 (Table 4). At 8 weeks after surgery, histologic scores were lower in group 2 compared with scores at 4 weeks (Table 5). Scores were significantly higher in group 3 than in group 2. At 8 weeks after surgery, group 2 showed a wider area of bony bridge formation, resulting in lower scores. Group 3 showed a thickened physeal area, resulting in higher scores.

DISCUSSION

The physis has limited ability to repair itself. Injury and damage may thus lead to deformities and shortening of long bones by growth arrest with bone bridge formation. Various treatments such as gradual correction and bone bridge resection have been used with varying rates of success. In treatment by bone bridge resection, several types of interposition material have been used in clinical practice. Langenskiold[21] reported 38 cases of physeal bridge resection using autogenous body fat, suggesting that 82% of cases benefited from the procedure. Bright reported a series of 100 patients treated using silastic as the interposition material,[22] with 81% of patients demonstrating some growth after bridge resection, and 70% achieving good to excellent results. Klassen and Peterson[23] reviewed the Mayo Clinic experience with 50 cases of physeal bridge resection using cranioplast (methylmethacrylate) as the interposition material, reporting early closure of the operated physis. These findings

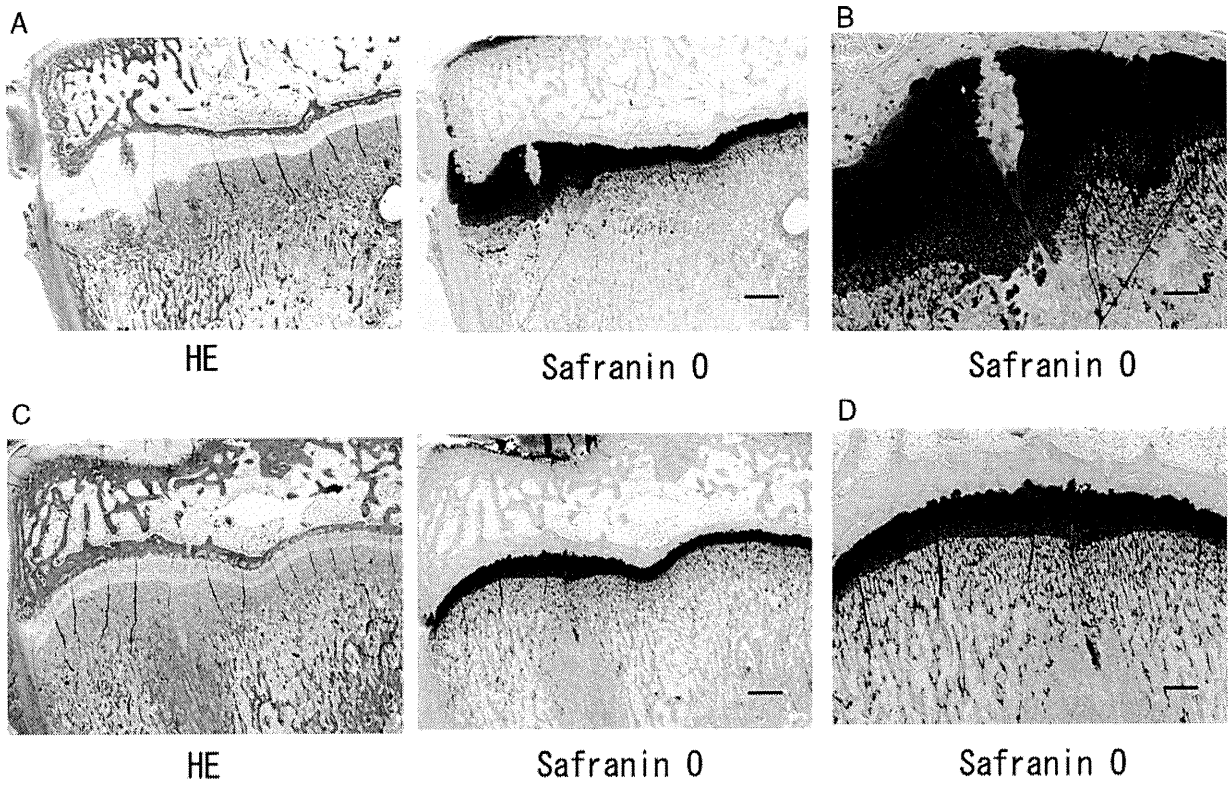

FIGURE 6. Histology in group 3 (TEC). A, Histology at 4 weeks after surgery, showing little bony bridge formation and repaired epiphyseal plate on the operated site. B, High-power section (×2) of the new physis at 4 weeks after surgery. Proliferative and prehypertrophic chondrocyte-like cells are seen on the operated site, and the physeal area is thickened. Bar, 500 μm. C, Histology at 8 weeks after surgery, showing repaired epiphyseal plate. D, High-power section (×2) at 8 weeks after surgery, showing the thickened physeal area on the operated site. Bar, 500 μm. HE indicates hematoxylin and eosin.

suggest that the interposition of fat, silastic, and other artificial materials might be associated with limitations to bone growth and several issues associated with long-term safety. We used bone wax as the interposition material in group 2. Many orthopaedic surgeons perform fat grafting in human epiphyseal plate injury. However , the bone wax is more difficult to be absorbed than the fat, and so, we used bone wax as the interposition material in this study.

The present study has demonstrated the feasibility of using a unique scaffold-free TEC from synovium-derived MSCs to repair the injured epiphyseal plate. The use of this unique TEC has the following benefits.

First, TECs can be autogeneously developed without any need for an exogenous scaffold. Implantation of TECs thus has minimal risk of potential side effects induced by biological and artificial materials in the scaffold. Some papers have reported transfer of MSCs using scaffolds for the treatment of growth arrest.[24,25] No similar reports in the literature have mentioned the use of cultured MSCs without scaffolds to repair epiphyseal plate injury.

Second, TECs have the ability to allow chondrogenesis. We implanted pluripotent MSCs into the epiphyseal plate area, because reconstructing the columnar structure of the growth plate by MSCs in vitro is difficult.

TABLE 4. Histologic Scores 4 Weeks After Surgery for the Repaired Growth Plate

Rabbit Number	Group 1	Group 2 (Bone Wax)	Group 3 (TEC)
1	0.0	1.0	3.0
2	0.5	2.5	3.0
3	0.5	3.0	3.5
4	4.0	6.0	3.5
5	5.5	8.5	5
6	—	—	6.5
7	—	—	7.0
Mean ± SD	2.1 ± 2.4	4.2 ± 3.0	4.5 ± 1.6

TEC indicates tissue-engineered construct.

TABLE 5. Histologic Scores 8 Weeks After Surgery for the Repaired Growth Plate

Rabbit Number	Group 1	Group 2 (Bone Wax)	Group 3 (TEC)
1	1.0	1.5	2.0
2	1.0	1.5	3.0
3	3.0	1.5	5
4	3.0	1.5	6.0
5	5.0	2.0	7.0
6	—	—	8.0
Mean ± SD	2.6 ± 1.6	1.6 ± 0.2	5.2 ± 2.5*

*Significantly different from groups 1 and 2 ($P < 0.05$).
TEC indicates tissue-engineered construct.

The local in vivo environment might have stimulated differentiation of the TEC. For example, multiple cytokines such as parathyroid hormone-related protein and Indian hedgehog exist at various concentration gradients in the growth plate. We hypothesized that these cytokines could help with regeneration of the injured physis. Our results showed that using MSCs without scaffolds resulted in less bony bridge formation and contributed to longitudinal bone growth. In the control group, bony bridge trabeculae replaced the epiphyseal plate. In the TEC group, proliferative and prehypertrophic chondrocyte-like cells were seen on the operated site. These cells took on a slightly disordered columnar arrangement like a normal physis, and the physeal area was thickened (Fig. 6). The implanted stem cells may thus show differentiation responses in the epiphyseal plate. In groups 2 and 3, the radiographic results were similar. However, the histologic scores of group 3 were significantly better than that of group 2. This is because the implanted stem cells could help the regeneration of the injured physis. We are planning to perform a longer duration of examination in the next study.

Further studies are needed to clarify the function of the new physis from the TEC with regard to bone growth and to examine applications in other large animals, including humans. This study used a small number of animals and only continued observations for 8 weeks. A larger number of subjects and a longer duration of examination are thus warranted. To attain more extensive chondrogenic differentiation responses, biological manipulation of the TEC may be required before implantation. This study used synovium-derived cells, which reportedly exhibit the most enhanced chondrogenic potential among mesenchymal tissue-derived cells.[11] If TECs are to be used for repair of epiphyseal injury in large animals such as humans, large quantities of cells will be needed. To overcome this problem, we are planning to use TECs cultured from induced pluripotent stem cells after confirming the quality of TECs developed using induced Pluripotent Stem cells in the next study.

CONCLUSIONS

A scaffold-free 3D TEC made using cultured synovium-derived MSCs differentiated into proliferative and prehypertrophic chondrocyte-like cells. We have demonstrated the feasibility of a scaffold-free 3D TEC as a new approach for the repair of epiphyseal injury.

REFERENCES

1. Langenskiold A. The possibilities of eliminating premature partial closure of an epiphyseal plate caused by trauma or disease. *Acta Orthopedica Scandinavica*. 1967;38:267–279.
2. Langenskiold A. An operation for partial closure of an epiphyseal plate in children, and its experimental basis. *J Bone Joint Surg Br*. 1975;57:325–330.
3. Broughton NS, Dickens DRV, Cole WG, et al. Epiphysiolysis for partial growth plate arrest. *J Bone Joint Surg Br*. 1989;71:13–16.
4. Langenskiold A. Surgical treatment of partial closure of the growth plate. *J Pediatr Orthop*. 1981;1:3–11.
5. Williamson RV, Staheli LT. Partial physeal growth arrest: treatment by bridge resection and fat interposition. *J Pediatr Orthop*. 1990;10:769–776.
6. Bright RW. Operative correction of partial epiphyseal plate closure by osseous-bridge resection and silicon-rubber implant. *J Bone Joint Surg Am*. 1974;56:655–664.
7. Macksoud WS, Bright R. Bar resection and silastic interposition in distal radial physeal arrest. *Orthop Trans*. 1989;13:1–2.
8. Pttenger MF, Mackay AM, Beck SC, et al. Multilineage potential of adult human mesenchymal stem cells. *Science*. 1999;284:143–147.
9. Jankowski RJ, Deasy BM, Huard J. Muscle-derived stem cells. *Gene Ther*. 2002;9:642–647.
10. Bari CD, Dell'Accio F, Tylzanowski P, et al. Multipotent mesenchymal stem cells from adult human synovial membrane. *Arthiritis Rheum*. 2005;44:1928–1942.
11. Sakaguchi Y, Sekiya I, Yagishita K, et al. Comparison of human stem cells derived from various mesenchymal tissues: superiority of synovium as a cell source. *Arthiritis Rheum*. 2005;52:2521–2529.
12. O'Grady JE, Bordon DM. Global regulatory registration requirements for collagen-based combination products: points to consider. *Adv Drug Deliv Rev*. 2003;55:1699–1721.
13. Hunziker EB. Articular cartilage repair: basic science and clinical progress. A review of the current status and prospects. *Osteoarthritis Cartilage*. 2002;10:432–463.
14. Hunziker EB, Rosenberg LC. Repair of partial-thickness defects in articular cartilage: cell recruitment from the synovial membrane. *J Bone Joint Surg Am*. 1996;78:721–733.
15. Lee CR, Grodzinsky AJ, Hsu HP, et al. Effects of a cultured autologous chondrocyte-seeded type II collagen scaffold on the healing of a chondral defect in a canine model. *J Orthop Res*. 2003;21:272–281.
16. Dorotka R, Bindreiter U, Macfelda K, et al. Marrow stimulation and chondrocyte transplantation using a collagen matrix for cartilage repair. *Osteoarthritis Cartilage*. 2005;11:877–886.
17. Nakamura N, Iwahashi T, Kawano K, et al. Healing of a chondral fragment of the knee in an adolescent after internal fixation. A case report. 2004. *J Bone Joint Surg Am*. 2004;86:2741–2746.
18. Ando W, Tateishi K, Hart DA, et al. Cartilage repair using an in vitro generated scaffold-free tissue engineered construct derived from porcine synovial mesenchymal stem cells. *Biomaterials*. 2007;28:5462–5470.
19. Ando W, Tateishi K, Katakai D, et al. In vivo generation of a scaffold-free tissue engineered construct (TEC) derived from human synovial mesenchymal stem cell: biological and mechanical properties, and future chondrogenic potential. *Tissue Eng Part A*. 2008;14:2041–2049.
20. Shimomura K, Ando W, Tateishi K, et al. The influence of skeletal maturity on allogenic synovial mesenchymal stem cell-based repair of cartilage in a large animal model. *Biomaterials*. 2010;31:8004–8011.
21. Langenskiold A. Surgical treatment of partial closure of the growth plate. *J Pediatr Orthop*. 1981;1:3–11.
22. Bright RW. Partial growth arrest: identification, classification, and results of treatment. *Orthop Trans*. 1982;6:65–66.
23. Klassen RA, Peterson HA. Excision of physeal bars: the Mayo Clinic experience 1968-1978. *Orthop Trans*. 1982;6:65.
24. Li L, Hui JH, Goh JC, et al. Chitin as a scaffold for mesenchymal stem cells transfers in the treatment of partial growth arrest. *J Pediatr Orthop*. 2004;24:205–210.
25. Chen FC, Hui JHP, Chan WK, et al. Cultured mesenchymal stem cell transfers in the treatment of partial growth arrest. *J Pediatr Orthop*. 2003;23:425–429.

人工骨による骨再生

吉川秀樹[*1]・名井陽[*2]

1．はじめに

整形外科では，さまざまな骨の疾患や外傷などで，骨の欠損が生じる．骨の腫瘍，骨折，人工関節のゆるみなどに対して，骨の欠損部を補い再生させるためには，自分の骨盤(腸骨)や下腿骨(腓骨)の一部から，骨を採取し移植する『自家骨移植』が古くから用いられてきた．骨の再生には，自家骨が最も優れているが，健康な部分にメスを入れ骨を採取するという難点がある．また，採取量に限界があること，骨採取部の術後の血腫，疼痛，骨折などの合併症を生じることなどが問題であった．また，骨粗鬆症(こつそしょうしょう)の患者では，採取する骨自体がもろいため，移植骨として有用ではない[1]．一方，1980年代から研究・開発されてきた人工骨は，健康な骨を傷つけることなく，十分な大きさの骨を再生させることが可能である．主な成分は，骨や歯の無機成分でもあるハイドロキシアパタイトなどの化合物で，人体に炎症や拒絶反応などの副作用は示さない[1,2]．本稿では，良好な骨再生能を有する人工骨の開発と，種々の整形外科疾患での臨床応用について解説する．

2．連通多孔体人工骨の開発

これまで人工骨として，ハイドロキシアパタイト，アルミナ，バイオグラスなどさまざまな素材が開発，使用されてきた[2~4]．中でも，骨の無機質の主成分であり骨と直接結合するハイドロキシアパタイト(hydroxyapatite；HA，水酸アパタイト，$Ca_{10}(PO_4)_6(OH)_2$)や生体内で吸収されるβリン酸三カルシウム(beta-tricalcium phosphate；βTCP，$Ca_3(PO_4)_2$)など，種々のバイオセラミックスによる人工骨が開発され，臨床応用されてきた．特に内部に“気孔”と呼ばれる小空隙を多数有する多孔体人工骨は，気孔内に新生骨が再生し母床骨と完全に同化することが期待され良好な臨床成績が報告されてきた[5,6]．さらに，1990年代以後に新たに開発されてきた多孔体セラミックス人工骨の多くは，製造方法の工夫などにより高気孔率(75~85%)かつ高い気孔間連通性を有しており，ほぼ全ての気孔が大きい径の気孔間連通孔でつながった構造を持つ[7,8]．これらの高気孔率，高連通性人工骨は生体骨内に埋植したあとの早期(数週間程度)で旺盛な気孔内骨形成が見られ，きわめて早期に母床骨と一体化する．著者らが，物質・材料研究機構との共同研究により“起泡ゲル化技術”を用い作製した連通多孔体ハイドロキシアパタイト(NEOBONE)は，走査電子顕微鏡所見で，ほぼ球形で比較的均一の気孔(気孔率75%，平均気孔径150 μm)が秩序良く配列し，互いに気孔間連通孔で連絡している(図1，図2)．連通孔径分布は10~80 μm(平均40 μm)にあり，気孔の90%が細胞や組織が十分通過できる大きさの連通孔でつながっており，気孔の内部に骨髄幹細胞，血管，BMPなどの増殖因子/サイトカインや遺伝子の導入が可能である[9~11]．力学的強度は初期圧縮強度で12 Mpaであり優れた数値を示した．ウ

[*1] Hideki Yoshikawa　大阪大学大学院医学系研究科器官制御外科学(整形外科)　教授　医学博士
[*2] Akira Myoui　大阪大学医学医学部附属病院未来医療センター　准教授　医学博士
Bone regeneration by bone substitutes

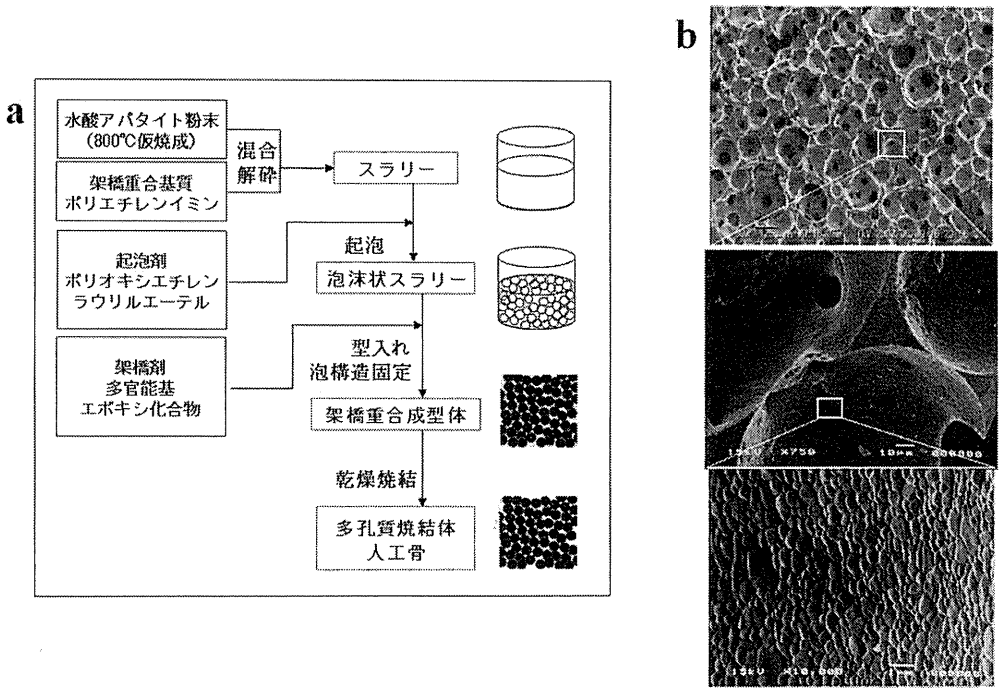

図1　連通多孔体人工骨(NEOBONE)の製法，構造
a：気泡ゲル化法による連通多孔体ハイドロキシアパタイト(NEOBONE)の製法，b：走査電顕像での内部構造

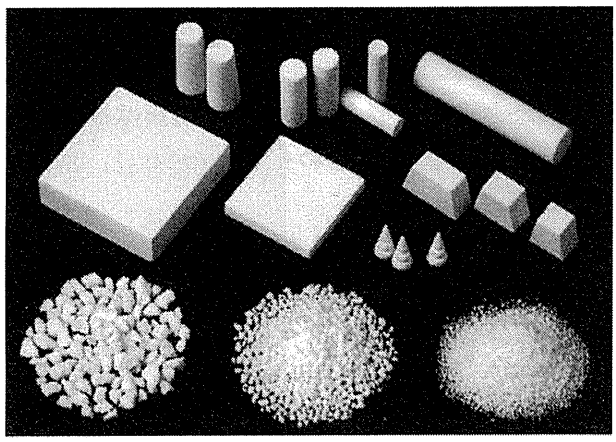

図2　連通多孔体人工骨(NEOBONE)の外観

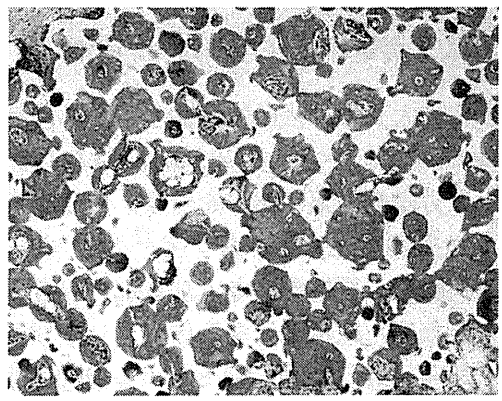

図3　ラット骨髄幹細胞/NEOBONE 複合体の筋肉内移植による骨再生(移植後6週の組織像，HE染色，×40)

サギ大腿骨にNEOBONEを移植した際に，移植後6週間で直径6 mmの円柱の深層にまで気孔間連通孔を経て，豊富な血管新生を伴う新生骨，新生骨髄が観察され，優れた骨再生能を示した．また，この骨新生に伴い圧縮強度は移植後9週で初期強度の3倍に達した[7]．

3．骨再生能を付加した人工骨の開発

連通構造を有する人工骨は，その優れた骨伝導能(骨細胞を内部に呼び込む能力)を呈するのみならず，気孔の内部に骨形成蛋白(BMP，bone morphogenetic protein)や骨髄幹細胞を導入し生物活性を有する人工骨の開発を可能にする．ラットより採取した新鮮骨髄幹細胞を培養し浮遊細胞を除去し，付着細胞を増殖させた後NEOBONEに含浸させ，それを同系ラット背部筋膜下に移植し異所性骨形成を観察した．移植後6週で，全ての気孔内に豊富な骨形成を観察することができた(図3)[9~11]．また，NEOBONE内に骨形成蛋白(BMP)を導入し，骨誘導活性(骨のない部位に骨組織を再生させる能力)を有する人工骨の開発を試みた．白色家兎橈骨に15 mmの骨欠損を作製し，rhBMP-2(5 or 20 μg)/PLA-PEG(20 mg)/NEOBONE複合体を同部に移植した．NEOBONE

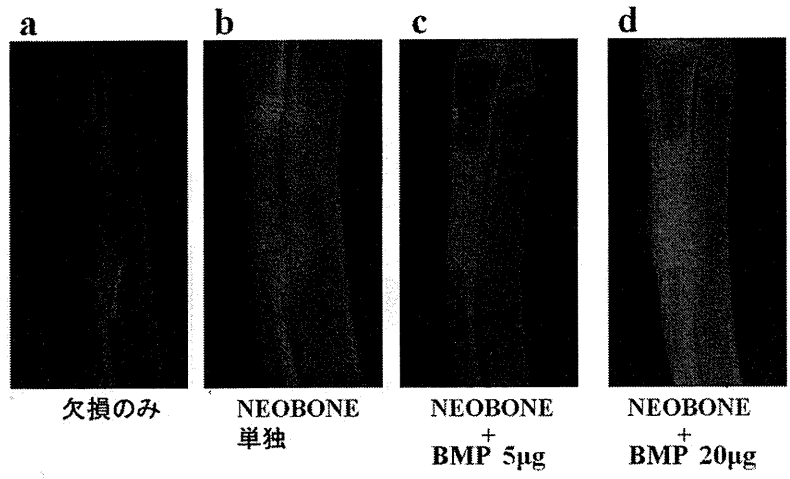

図４　ウサギ前腕骨欠損部の NEOBONE による骨再生(移植後 5 週の軟 X 線像)
a：骨欠損のみ，b：NEOBONE 単独，c：rhBMP-2(5 μg)/PLA-PEG(20 mg)/NEOBONE 複合体，d：rhBMP-2(20 μg)/PLA-PEG(20 mg)/NEOBONE 複合体

単独群では，インプラントと host bone の間に明らかなレントゲン透亮像を認めたが，BMP 群では，術後 5 週までにインプラントと骨の癒合を認め，組織学的にも，内部に旺盛な骨および骨髄組織の形成を認めた(図４)[10~12].

４．人工骨を用いた整形外科手術

連通多孔体人工骨は，動物実験でも優れた骨再生能を示したことから，臨床治験が行われ，2003 年の厚生労働省の薬事認可を受け，現在まで一万例以上の症例に使用されている[13~15]．さらに，大腿骨，脛骨，脊椎椎体など加重部位の骨再生に対応するため，緻密体と多孔体のコンポジット人工骨の開発(NEOBONE-X)を行い，2009 年発売されている(図５)[16]．整形外科の種々の疾患に対して使用された症例を供覧する．

・14歳，男子，単発性骨嚢腫(図６)

野球で投球した後，右肩激痛が出現し，続行不能となった．単純 X 線により，右上腕骨の骨溶解像を認めた(図６a)．術中所見では，骨皮質は菲薄化し，内部は漿液性で，骨髄は欠損していた．顆粒状人工骨(NEOBONE)を充填し，自家骨移植は行わなかった(図６b)．術後３ヵ月の単純X線像では，術直後に見られた顆粒状陰影はほぼ消失し，豊富な骨再生が認められた(図６c)．術後３年，再発を認めない．

・65歳，女性，関節リウマチ(図７)

７年前に発症した関節リウマチで，治療中，右膝関節の疼痛が著明となった．単純X線では，膝関節の骨破壊，関節裂隙の消失，脛骨近位中央部の巨大な嚢腫様変化を認めた(図７a-b)．この状態での人工膝関節の設置は不安定であるため，骨

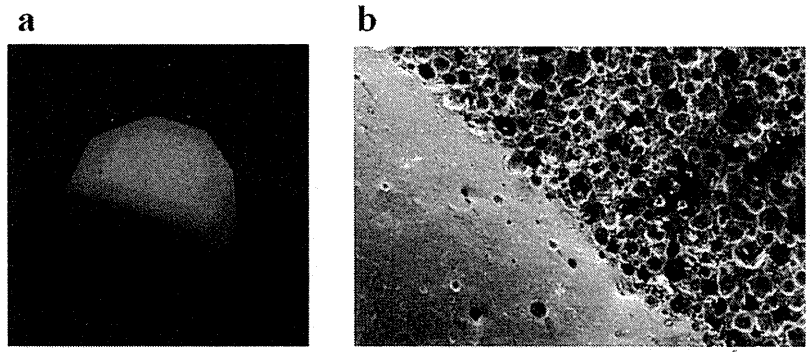

多孔体部: porosity: 75%, 12 MPa
緻密体部: porosity: 0%, 570 MPa

図５　緻密体と多孔体のコンポジット人工骨(緻密体：570Mpa，多孔体：12 Mpa)
a：肉眼像，b：走査電顕像での内部構造

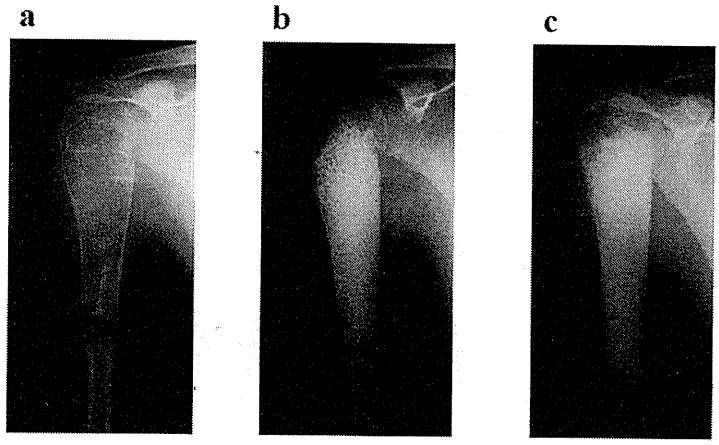

図6　右上腕骨骨嚢腫
a：術前の単純X線像，b：術直後のX線像，c：術後3ヵ月のX線像

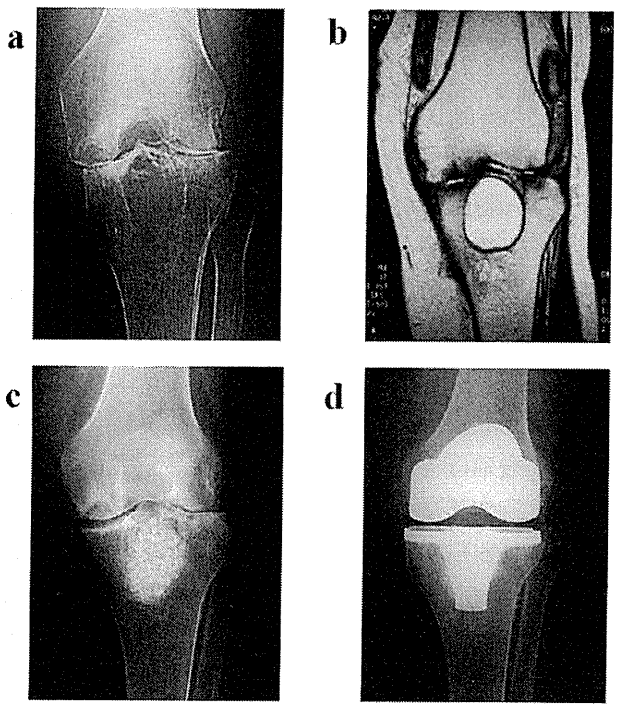

図7　左膝関節，関節リウマチ
a：術前の単純X線像，b：MRI像，c：人工骨移植術後の単純X線像，d：人工関節置換術後の単純X線像

破壊の進行予防，病的骨折予防の目的で，まず脛骨骨嚢胞に対し，人工骨移植術を施行した(図7c)．術後6ヵ月で，良好な骨再生が確認されたため，この時点で人工膝関節全置換術を施行した(図7d)．術後3年，人工関節のゆるみも生じず，経過良好である．

5. テーラーメイド人工骨の開発：CAD/CAM技術による形状の制御

通常の多孔体人工骨は，直径数mm程度の顆粒か，数cm程度の大きさの円柱や立方体など汎用形状品(ブロック体)，あるいは使用する部位や手術に合わせた既製のサイズ形状の特殊形状品として供給されている(図2)．しかし高気孔率，高連通性人工骨が利用できるようになると，新たな方法でブロック体人工骨を活用できる可能性が出てきた．その一つが，一人一人の患者の病態にあわせて最適な形状のブロック体人工骨を作成する“テーラーメイド人工骨”である．術前にあらかじめ最適な形状に加工しておいた人工骨が利用できれば，手術の精度が向上し，手術時間を短縮できるなど，メリットが大きい．三次元CADデータを元に，コンピュータ制御で三次元モデルを作成するCAM(computer-aided manufacturing)の方法を用いてモックを作成することが可能である．著者らは，医療現場で比較的簡単に導入可能でかつ，セラミックスを扱える方法として切削ラピッドプロトタイピングに注目し，臨床応用を試みている[17,18]．たとえば，骨折後の変形治癒などで骨の角度を矯正する必要があるとき“矯正骨切り術”が施行される．自家骨を移植片として用いるくさび開き矯正骨切術では，術中に移植片の形態の加工する必要があるため正確な移植片を得ることが困難である．図8は48歳女性，橈骨遠位端骨折の変形治癒であるが，術前のCTから再構成した3次元画像において，楔開き骨切り術のシミュレーションを行い，楔状の移植片の形状を決定した．この形状の三次元データに基づき，3次元切削モデリング装置(3Dプロッタ MODELA MDX-20，ローランドDG社製)を使ってNEOBONEの直方体ブロックから移植用の楔状ブロック体を削

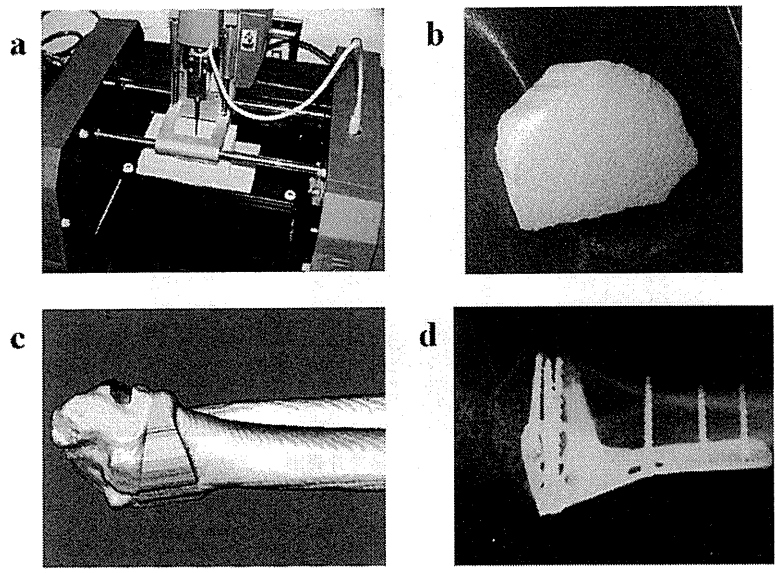

図8　CAD/CAM 技術による NEOBONE の形状最適化
a：コンピュータデータ入力切削器を用いた NEOBONE の加工，b：加工済み NEOBONE，
c：矯正骨切術の計画，骨欠損部の再構成，d：術後 6 ヵ月の単純 X 線像

り出した．本法で作成した楔状ブロックは，術中一切加工せずに骨切部にフィットし正確な矯正が得られた．10ヵ月後のレントゲン像では移植したブロックの圧潰はなく矯正位が保たれ，完全な骨癒合が得られた．

6．人工骨をスカフォールドとして用いた骨再生医療

高気孔率高連通性セラミックス人工骨の気孔には，血管や新生骨など再生に必要な組織の侵入が容易なだけでなく，液体に浮遊させた細胞の導入が容易である．著者らは大阪大学医学部附属病院未来医療センターの細胞培養調整施設を利用し，良性骨腫瘍および骨腫瘍類似疾患の患者を対象に，「自家骨髄由来培養細胞導入人工骨による骨疾患の治療臨床試験」を 8 例に実施した[19,20]．局麻下に骨髄穿刺を行い，患者骨盤より 15～50 ml の骨髄液を得る．骨髄細胞を 15％自己血清を含むαMEM 培地で 2 ～ 3 週間ほど培養すると，紡錘形の付着性細胞が増殖してくる．この細胞は約 90％が増殖能と骨芽細胞など間葉系細胞への分化能を維持する間葉系幹細胞である，この細胞の浮遊液に，NEOBONE を一晩浸すと気孔内に細胞が導入され気孔壁に付着する．これをさらに約 2 週間，アスコルビン酸，β-グリセロリン酸，デキサメサゾンを添加した15％自己血清を含む

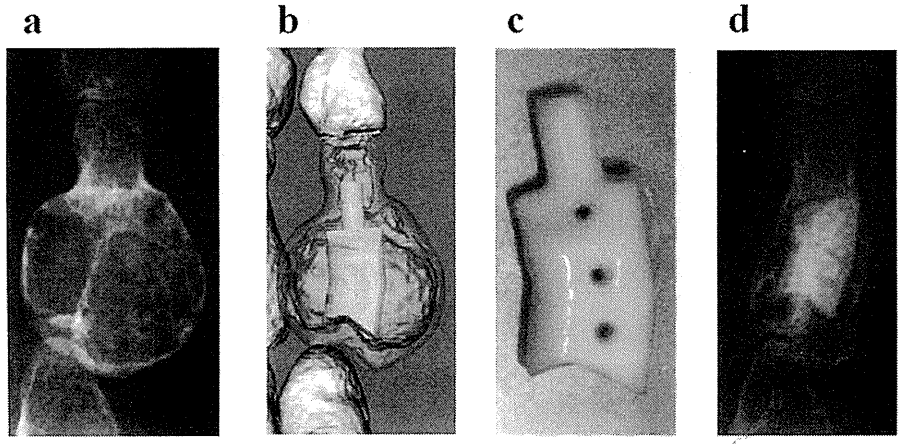

図9　自家培養間葉系細胞導入人工骨による骨腫瘍の治療
手指内軟骨腫
a：術前の単純 X 線像，b：患部の CT 像より作製した腫瘍切除後の骨欠損の 3 次元モデルと人工骨デザイン，
c：自家骨髄由来間葉系細胞導入人工骨，d：移植後 10 ヵ月の単純 X 線像

αMEM で培養し骨芽細胞へ分化誘導したのち，手術で骨欠損部に移植している．図9は18歳男性で，多発性内軟骨腫症のため，両手指に多数の骨性隆起を認めた．右示指の骨腫瘍を切除し，前述のテーラーメイド人工骨を足場として患者自己骨髄由来間葉系細胞導入人工骨を作成し欠損部に移植した．術後10ヵ月で，良好な変形治癒，骨再生を認め，患者満足度は高かった．この方法は将来的には，骨形成にとって極めて不利な条件の病巣，たとえば悪性腫瘍切除後や外傷・骨髄炎などによる巨大な骨欠損を機能的に再建するための新しい治療法として期待される．

7. おわりに

近年，種々の人工骨の開発が進められ，骨の再生技術が飛躍的に発展しつつある．骨再生能力に富む，連通多孔体人工骨の登場により，骨盤などから自家骨の採取が不要となり，低侵襲手術が可能となった．また、骨欠損部の形状を術前に切削加工が可能であることから，テーラーメイド型骨移植材料として臨床応用が進められている．さらに、自家骨髄間葉系細胞導入人工骨は，外傷，腫瘍などによる大型骨欠損の修復には非常に有用性の高い技術となる可能性がある．骨再生医療に対する社会的要請，医学界および産業界からの期待は大きく，近い将来，人工骨を用いた骨組織の再生医療が実現されるものと思われる．

文　献

1) 吉川秀樹，名井　陽: 骨移植と人工骨，Current Therapy, 21:48-51, 2003.

2) Uchida A, Araki N, Shinto Y, Yoshikawa H, Kurisaki E, Ono K: The use of calcium hydroxyapatite ceramic in bone tumour surgery. J Bone Joint Surg, 72B: 298-302, 1990.

3) Akao M, Aoki H, Kato K: Mechanical properties of sintered hydroxyapatite for prosthetic application. J Mater Sci, 16: 809-812, 1981.

4) Nakamura T, Yamamuro T, Higashi S, Kokubo t, Itoo S: A new glass-ceramic for bone replacement: evaluation of its bonding to bone tissue. J Biomed Mater Res, 19:685-98, 1985.

5) Matsumine A, Myoui A, Kusuzaki K, Araki N, Seto M, Yoshikawa H, Uchida A: Calcium hydroxyapatite ceramic implants in bone tumour surgery. A long-term follow-up study. J Bone Joint Surg Br, 86:719-25, 2004.

6) Ogose A, Kondo N, Umezu H, Hotta T, Kawashima H, Tokunaga K, Ito T, Kudo N, Hoshino M, Gu W, Endo N: Histological assessment in grafts of highly purified beta-tricalcium phosphate (Osferions) in human bones. Biomaterials, 27: 1542–9, 2006

7) Tamai N, Myoui A, Tomita T, Nakase T, Tanaka J, Ochi T, Yoshikawa H: Novel hydroxyapatite ceramics with an interconnective porous structure exhibit superior osteoconduction in vivo. J Biomed Mater Res, 59: 110-117, 2001.

8) Sakamoto M, Nakasu M, Matsumoto T, Okihana H: Development of superporous hydroxyapatites and their examination with a culture of primary rat osteoblasts. J Biomed Mater Res, 82A:238-42, 2007.

9) Nishikawa M, Myoui A, Ohgushi H, Ikeuchi M, Tamai N, Yoshikawa H: Bone tissue engineering using novel interconnected porous hydroxyapatite ceramics combined with marrow mesenchymal cells: Quantitative and three-dimensional image analysis / ceramic construct: comparison with marrow mesenchymal cell/ ceramic composite. Cell Transplant, 13: 367-376, 2004.

10) Yoshikawa H, Myoui A: Bone tissue engineering with porous hydroxyapatite ceramics. J Artif Organs, 2005, 8:131-136.

11) 名井　陽，吉川秀樹：連通多孔体型ハイドロキシアパタイトの開発と再生医療への展開，骨・関節・靭帯，17:1205-1215, 2004.

12) Kaito T, Myoui A, Takaoka K, Saito N, Nishikawa M, Tamai N, Ohgushi H, Yoshikawa H: Potentiation of the activity of bone morphogenetic protein-2 in bone regeneration by a PLA-PEG/hydroxyapatite composite. Biomaterials, 26:73-79, 2005.

13) 玉井宣行，名井　陽，荒木信人，秋田鐘弼，中瀬尚長，海渡貴司，村瀬剛，上田孝文，越智隆弘，吉川秀樹：新規全気孔連通型 HA 多孔体 NEOBONE を用いた骨欠損に対する治療，関節外科，23:100-107, 2004.

14) 名井　陽，玉井宣行，荒木信人，藤井昌一，冨田哲也，古野雅彦，吉川秀樹：連通気孔構造を有するハイドロキシアパタイト人工骨の臨床応用、物理学的特性・臨床的特徴・問題点，日整会誌，80:262-269, 2006.

15) Tamai N, Myoui A, Kudawara I, Ueda T, Yoshikawa H: Novel fully interconnected porous hydroxyapatite ceramic in surgical treatment of benign bone tumor. J Orthop Sci, 15:560-8, 2010.

16) Kaito T, Mukai Y, Nishikawa M, Ando W, Yoshikawa H, Myoui A: Dual hydroxyapatite composite with porous and solid parts: Experimental study using canine lumbar interbody fusion model. J Biomed Mater Res, 2006, 78B:378-84.

17) 村瀬剛，森友寿夫，後藤晃，吉川秀樹: 肘過伸展外反変形に対して 3D コンピューターシミュレーションを用いて尺骨矯正骨切り術を行った一例．日本肘関節学会雑誌，11: 53-54, 2004.

18) 岡久仁洋，村瀬剛，森友寿夫，後藤晃，吉川秀樹: 3D-CAD モデルによるハイドロキシアパタイトインプラントの術前モデリングと 3 次元矯正骨切り術．中部整災誌，50:141-142, 2007.

19) 名井　陽，吉川秀樹: 骨の再生．最新整形外科学大系，第3巻「運動器の治療学」，越智隆弘編，中山書店，364-369, 2009.

20) 橋本伸之，名井　陽，吉川秀樹: Ollier 病による手指変形に対するカスタムメイド人工骨の使用経験，中部整災誌，53:123-124, 2010.

Cardiovasc Drugs Ther (2012) 26:409–416
DOI 10.1007/s10557-012-6410-4

Design and Rationale of Low-Dose Erythropoietin in Patients with ST-Segment Elevation Myocardial Infarction (EPO-AMI-II Study): A Randomized Controlled Clinical Trial

Tetsuo Minamino · Ken Toba · Shuichiro Higo · Daisaku Nakatani · Shungo Hikoso · Masao Umegaki · Kouji Yamamoto · Yoshiki Sawa · Yoshifusa Aizawa · Issei Komuro · EPO-AMI-II study investigators

Published online: 2 September 2012

Abstract
Purpose The development of novel pharmaceutical interventions to improve the clinical outcomes of patients with acute ST-segment elevation myocardial infarction (STEMI) is an unmet medical need worldwide. In animal models, a single intravenous administration of erythropoietin (EPO) during reperfusion improves left ventricular (LV) function in the chronic stage. However, the results of recent proof-of-concept trials using high-dose EPO in patients with STEMI are inconsistent. In our pilot study, low-dose EPO after successful percutaneous coronary intervention (PCI) improved the LV ejection fraction (EF) and did not trigger severe adverse clinical events in patients with STEMI. One possible reason for this discrepancy is the dose of EPO used.
Methods and results We have started a double-blind, placebo-controlled, randomized, multicenter clinical trial (EPO-AMI-II) to clarify the safety and efficacy of low-dose EPO in patients with STEMI. STEMI patients who have a low LVEF (<50 %) will be randomly assigned to intravenous administration of placebo or EPO (6,000 or 12,000 IU) within 6 h after successful PCI. The primary endpoint is the difference in LVEF between the acute and chronic phases (6 months), as measured by single-photon emission computed tomography. The patient number needed for EPO-AMI-II is 600. The study will stop when superior efficacy or futility is detected by an interim analysis. This study has been approved by the Evaluation System of Investigational Medical Care.
Conclusions EPO-AMI-II study will clarify the safety and efficacy of low-dose EPO in STEMI patients with LV dysfunction in a double-blind, placebo-controlled, multicenter study. (247 words)

Key words Erythropoietin · Low-dose · Acute myocardial infarction · LV dysfunction

Names of Grants: Grants-in-Aid from the Ministry of Health, Labour and Welfare (Japan); the Ministry of Education's Support and Training Program for Translational Research at Osaka University; and the Japanese Circulation Society Grant for Translational Research 2010

T. Minamino · S. Higo · D. Nakatani · S. Hikoso · Y. Sawa · I. Komuro (✉)
Department of Cardiovascular Medicine,
Osaka University Graduate School of Medicine,
2-2 Yamada-oka,
Suita, Osaka 565-0871, Japan
e-mail: komuro-tky@umin.ac.jp

K. Yamamoto
Department of Biomedical Statistics,
Osaka University Hospital,
Suita, Japan

M. Umegaki
Medical Center for Translational Research, Osaka University Hospital,
Suita, Japan

K. Toba
First Department of Internal Medicine,
Niigata University Medical and Dental Hospital,
Niigata, Japan

Y. Aizawa
Tachikawa Medical Center,
Nagaoka, Japan

Despite improved clinical outcomes by early reperfusion with thrombolysis and primary percutaneous coronary intervention (PCI) with stenting, the mortality of patients with

ST-segment elevation myocardial infarction (STEMI) is still high in Western countries and Japan [1, 2]. Furthermore, in the chronic stage after MI, heart failure can develop due to left ventricular (LV) remodeling [3]. To date, most clinically tested agents that induce cardioprotection have failed to reduce infarct size in clinical settings [4]. Thus, novel pharmaceutical interventions to improve the clinical outcomes of patients with STEMI are urgently needed. Animal studies show that the intravenous administration of erythropoietin (EPO), a glycoprotein hormone consisting of 165 amino acid residues [5], at the onset of reperfusion reduces the myocardial infarct size and prevents cardiac remodeling, with enhanced neovascularization in the heart after MI [6, 7]. Several proof-of-concept studies have been performed to clarify the cardioprotective effects of EPO in patients with STEMI. The administration of high-dose EPO (60,000–99,000 IU) did not improve left ventricular ejection fraction (LVEF) or reduce infarct size [8–10]. Regarding secondary endpoints, the use of EPO has been associated with a trend toward an increase in major adverse cardiovascular events in 2 studies [8, 10] and significantly fewer events in a third study [9]. In contrast, low-dose EPO is likely to be cardioprotective, according to small clinical trials [11–13]. Platelet activation by high-dose EPO [14] and the existence of an optimal dose for limiting infarct size [15] may explain the dose-dependent discrepancy of EPO-induced cardioprotection. Importantly, pilot studies showed that low-dose EPO is associated with improved left ventricular function without major adverse cardiovascular events [11, 12]. Furthermore, our post-hoc analysis revealed that EPO administration was highly associated with improved LV function in STEMI patients with a low LV ejection fraction (LVEF) (<50 %) (Fig. 1). Therefore, we have started a double-blind, placebo-controlled, randomized, multicenter clinical trial (EPO-AMI-II) to clarify the safety and efficacy of low-dose EPO in STEMI patients with a low LVEF (<50 %). The protocol was submitted to the Evaluation System of Investigational Medical Care of the Ministry of Health, Labour and Welfare of Japan and was approved under the Japanese governmental health insurance system on 1 August 2011.

Methods

Study objects

The objectives of this study are to evaluate whether a single bolus administration of EPO prevents ischemia-reperfusion injury dose-dependently and to estimate the optimum clinical dose of EPO in patients with STEMI after successful PCI by analyzing the improvement in LVEF between the acute and chronic stages.

Study design

EPO-AMI-II is an ongoing multicenter, prospective, randomized, double-blind, placebo-controlled, dose-finding study in patients presenting with a first STEMI. After a successful PCI, patients will be randomly assigned to receive either an intravenous bolus dose of epoetin-beta (EPO) (6,000 or 12,000 IU) or placebo on top of standard medical care (Fig. 2). This trial was registered at the UMIN Clinical Trials Registry as UMIN000005721.

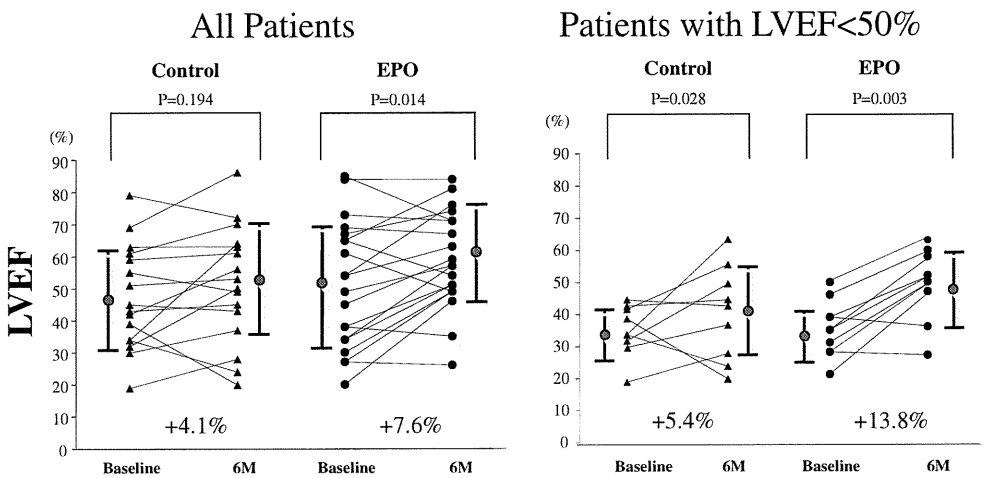

Fig. 1 Post-hoc analysis of the EPO-AMI-I results. Panel **a** shows the LVEF between the acute and chronic stages in all patients in the EPO-AMI-I study. EPO, but not saline, administration significantly increased LVEF at 6 months after an MI. Panel **b** shows the LVEF between the acute and chronic stages in patients with LVEF <50 % in the EPO-AMI-I study. Both saline and EPO significantly increased LVEF at 6 months after an MI. The improvement of LVEF did not significantly differ between the saline- and EPO-treated groups. See the abbreviation definitions in the text

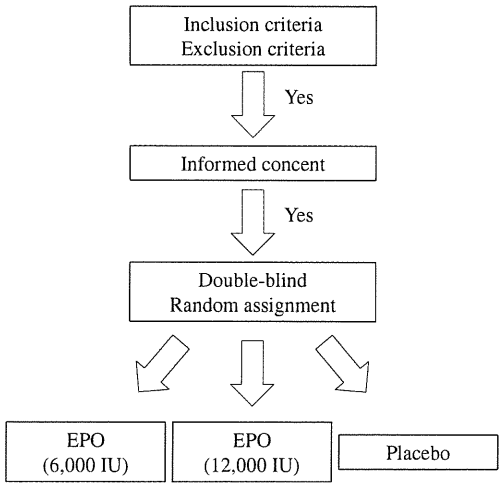

Fig. 2 Study flow chart

Patients

Consecutive patients with diagnostic signs and symptoms of an acute MI who satisfy the study inclusion and exclusion criteria (Table 1). After successful PCI, patients will be asked for written informed consent, and if they agree, will be assigned according to a pre-defined central web-based randomization system to receive EPO or placebo on top of optimal standard medical care. Patients will receive the study drug within 6 h after PCI. The patient, the attending physician, and the staff performing SPECT and the clinical follow-up will be unaware of the assigned treatment.

End points

The primary end point of this study is to evaluate the LVEF improvement between the acute (days 4–7) and chronic stages (6 months) (Table 2). The secondary end points of this study are to evaluate the efficacy and safety of EPO treatment. The efficacy is evaluated by analyzing indices of cardiac function 6 months after EPO administration. These are calculated with electrocardiogram-gated single-photon emission computed tomography (SPECT) and include LV end-diastolic volume (LVEDV), LV end-systolic volume (LVESD), LVEDV index, LVESV index, regional wall motion score, % uptake at resting, and defect size. The survival ratio, cardiovascular events (defined as cardiac death, stroke, nonlethal myocardial infarction, admission due to worsening of heart failure or unstable angina, revascularization, and onset of heart failure symptoms), and NT-ProBNP at the 6-month follow-up will also be analyzed to evaluate the efficacy of EPO treatment (Table 2). The safety is based on the incidence of major adverse events, clinical laboratory test data and vital signs.

Table 1 Inclusion and exclusion criteria

Inclusion criteria
1. Patients with first-time myocardial infarction
2. Patients with ST-elevation acute myocardial infarction (AMI) who have successful reperfusion by PCI within 12 h after the symptom onset
3. Patients whose ejection fraction at enrollment is <50 % on UCG or LVG
4. Age: over 20 years old, under 80 years old
5. Patients who agreed with participation to the trial in writing
Exclusion critetia
1. Patients with significant stenotic lesions in non infarct-related artery which require revascularization
2. Patients who resulted in obviously impaired reperfusion
3. Patients with Killip class III or IV, or cardiogenic shock at admission
4. Patients with advanced renal or hepatic dysfunction (Cre more than 2 mg/dl, or T-Bil more than 3 mg/dl)
5. Patients with blood pressure more than 140/90 mmHg after PCI
6. Hematocrit more than 54 % on admission
7. Patients who exhibit atrial fibrillation after PCI
8. Patients who have been diagnosed with malignant hypertension
9. Patients who have previously received treatment with EPO
10. Patients who received a blood transfusion in the last 3 months
11. Patients who are or have been diagnosed with cancer in the past 5 years
12. Patients who are complicated with severe infection such as pneumonia or sepsis
13. Patients who are contraindicated to aspirin or thienopyridine derivatives
14. Women who are pregnant, breastfeeding, or have a possibility for pregnancy
15. Patients whom researchers judged that they are not appropriate to participate this trial

Study drug administration

Prior to or at the time of primary PCI, standard antithrombotic treatments for acute MI are administered. Within 6 h after PCI, the enrolled patients are randomly assigned to placebo or an Epo dose (6,000 or 12,000 IU). Active drug or placebo is diluted in 10 mL of saline and administered intravenously over 1 min. The double-blind administration is ensured by a subject identification code unknown to physicians, nurses and patients. Drug or placebo is prepared under medical supervision according to instructions contained in predefined packages provided by the EPO-AMI-II organization. Standard treatment, including beta-blockade, lipid-lowering therapy, and angiotensin-converting enzyme inhibition or angiotensin-II receptor blockade, is additionally prescribed. EPO and placebo are kind gifts of Chugai Pharmaceutical Co. Ltd (Tokyo, Japan).

Table 2 Primary and secondary end points

Primary end point
The improvement of left ventricular ejection fraction at the chronic phase (the mean of differences between LVEF value at 4–7 days and that at 6 months after administration)
Secondary end point
[Efficacy]
1. Indexes of cardiac function 6 months after administration of epoetin-beta, which are calculated with cardiac scintigraphy (LVEDV, LVESV, LVEDVI, LVESVI, regional wall motion score, ischemia and defect size (SRS (Summed rest Score), SDS (Summed difference Score), %Defect Size, %uptake at resting))
2. Survival ratio
3. Cardiac event ratio (Cardiac death, stroke, nonlethal myocardial infarction, admission due to worsening of heart failure or unstable angina, revasculization, onset of heart failure symptoms (typical dyspnea at rest or during exercise, pulmonary congestion or pretibial edema)
4. NT-ProBNP 6 months after administration
[safety]
1. Adverse events
2. Laboratory test data
3. Vital signs (blood pressure, pulse rate)

Clinical and laboratory measures

Blood pressure, heart rate, and ECG are monitored at regular intervals until discharge (Fig. 3). Major adverse events (as defined above) are recorded during hospitalization and up to 6 months thereafter. At 4–7 days after admission and at 6 months, cardiac SPECT is also performed to evaluate cardiac function.

Quantification of LV function and infarct size

We will perform ECG-gated 99mTc-MIBI SPECT 4–7 days after PCI as the baseline measurement and at the 6-month follow-up. The 99mTc-MIBI (600–740 MBq) is administered at baseline and at the 6-month follow-up. SPECT image acquisition is performed 60 min after the 99mTc-MIBI injection. ECG-gated SPECT is performed after the administration of 99mTc-MIBI at rest. In ECG gating, SPECT data divided into 16 equal intervals are analyzed using Quantitative Gated SPECT software (Cedars-Sinai Medical Center, Los Angeles, CA, USA), which is also used to calculate EDVI, ESVI and LVEF. Pharmacologic stress tests are performed with non-gated 99mTc-MIBI SPECT. Adenosine (Adenoscan; DAIICHI SANKYO, Tokyo, Japan) is administered at a rate of 0.72 mg/kg for 6 min. The 99mTc-MIBI is injected 3 min after the start of adenosine infusion. The non-gated SPECT image is used to assess the severity of myocardial perfusion abnormalities, and regional uptake and the infarct area are calculated using Quantitative Perfusion SPECT software (Cedars-Sinai Medical Center). Regional uptake is assessed by applying a 17-segment model of the left ventricle according to the standard myocardial segmentation of the Cardiac Imaging Committee of the Council on Clinical Cardiology of the American Heart Association. Regional uptake is expressed as the mean uptake count in these segments. Defects at less than the threshold of 60 % of peak counts are identified as infarcted myocardium, and the infarct area is expressed as a percentage of the entire left ventricle involved. SPECT data will be analyzed in a blinded fashion by the SPECT Core Center members with the assistant of nuclear medicine special radiological technologist at MICRON Co., Ltd (Molecular Imaging CRO Network, Tokyo, Japan.). Finally, the analyzed data will be evaluated by an independent RI assessment committee.

Adverse events and additional safety assessments

An independent data safety monitoring board (DSMB) will receive real-time clinical information and will perform interim safety and efficacy analyses at 33 %, 66 % and 100 % recruitment. There are no formal (statistical) rules for stopping treatment due to safety reasons in this study. The DSMB recommendations are based on a clinical assessment of the frequency, and the nature of the serious adverse events and their relation to the investigational treatment.

Sample size calculation

Based on the results of our pilot study in STEMI patients with LVEF <50 % (LVEF improvement in the EPO-II group: 13.80±9.85 %, n=11, and in the placebo group: 5.44±14.80 %, n=9) (Fig. 1), the difference in LVEF improvement between the EPO (12,000 IU) treatment group and the placebo group is estimated to be 4.42 % with a common standard deviation of 14.33 %. As a result, the effect size is estimated to be 0.31 [16]. To demonstrate the

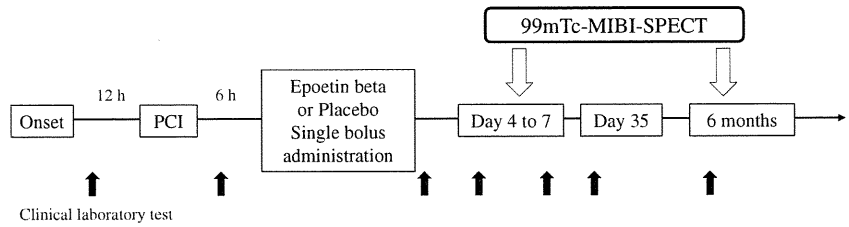

Fig. 3 Study schedule